CBS TECHNOLOGY CENTER

MODEL ANALYSIS OF A FORCE-DEFORMATION CHARACTERISTIC OF A PIANO HAMMER

FEBRUARY 25, 1985

By: Hideo Suzuki
CBS Technology Center
227 High Ridge Road
Stamford, CT 06905

MODEL ANALYSIS OF A FORCE-DEFORMATION CHARACTERISTIC OF A PIANO HAMMER

SUMMARY

Effects of a geometry and a Young's modulus profile of a piano hammer on its static force-deformation characteristic are studied using a finite-element model. The material properties of the model are assumed to be linear as well as isotropic. Therefore, only a geometrical nonlinearity is considered. A hammer model with a representative geometry and Young's modulus profile of an actual bass hammer has a force(f)-deformation(d) relationship approximated by a function, $f = A\ d^B$, with approximately $B = 1.67$. On the other hand, the degree of nonlinearity (B) of a particular bass hammer obtained from a dynamic measurement is approximately 2.3 or larger. A hammer with a larger increase of Young's modulus in the inward direction has a larger degree of nonlinearity. The geometry of a hammer has a large effect on the value, A, of the formula shown above. A hammer with a shorter height (distance from the top of the hammer to the top of the wood piece) or with a larger width has a larger value of A (in other words, a larger stiffness).

I. INTRODUCTION

One of the interesting properties of a piano tone is that a piano sounds brighter when a key is hit harder. This nonlinear phenomenon seems to be caused mostly by the nonlinear characteristic of a piano hammer. The stiffness and effective mass of the hammer significantly affects the interaction between the hammer and the string. A stiffer hammer bounces back quickly and the force applied to the string becomes more impulsive (a short contact time and a larger peak force), exciting the string with higher levels for higher-order harmonics. It is known that the hammer becomes stiffer and stiffer as it is deformed more and more.[1-3] The force (f) and the deformation (d) relationship may be approximated by:

$$f = Ad^2 + Bd^3 + Cd^4 \qquad (1)$$

or $$f = A\, d^B \qquad (2)$$

where A, B, and C are constants. (The reason why Eq. (1) has the orders of 2 or larger is that the stiffness of the hammer is effectively zero for a very small d.) Two reasons are considered for the nonlinearity of this kind. The first one is a material nonlinearity and the second one is a geometrical nonlinearity. Since the hammer is made of felt (wool) covering a wood piece, it may have a large degree of material nonlinearity. The geometrical nonlinearity is mostly caused by the increase of the contact area between the string and the hammer as the deformation of the hammer increases. Even if the felt material does not have a nonlinear property, the force-deformation relationship will be nonlinear due to the three-dimensional shapes of the hammer and the string.

The present paper discusses the nonlinearity of stiffness of a model hammer due to the geometrical nonlinearity. It is assumed that the material properties are linear as well as isotropic. The effects that the Young's modulus profile and the geometry of the hammer have on the force-deformation relationship will be discussed. The finite element program used to solve the present problem was supplied by Takehiko Kato . He was a consultant for this specific project from June 1, 1983 to August 31, 1983.

II. HAMMER MODEL

A. Geometry of the Model

The most laborious part of work using a finite element program is the generation of input data for a complex three-dimensional structure. Since we are not interested in investigating a particular piano hammer, we will use an ideal hammer model with a simplified geometry. The geometry of the finite element model is shown in Fig. 1. Only a quarter of the model is shown because the hammer is symmetric. The x-, y-, and z-coordinates are taken in the width, height, and thickness directions, respectively. Since the wood piece is much stiffer than felt, it is not included in the model and the boundary of felt facing the wood piece is considered fixed in all three directions. The wood piece is assumed to have a rectangular and constant cross section except for its top portion. The curved top portion is represented as part of an ellipse. The outer perimeter of felt, when looking into the x-y plane, is also represented by an ellipse. Because of the symmetry, the movement of the nodes on the x-y plane in the z-direction, and on the y-z plane in the x-direction is prohibited. In this simplified hammer model, the shape is determined by only five parameters, A_0, A_1, B_0, B_1, and the one-half thickness T. This simplifies the writing of a program to generate input data. The maximum number of elements is limited to 500 in the present program and, therefore, felt is divided into fairly small numbers of layers in its depth and width (five and seven, respectively). The program allows us to use only five different material properties. Areas with same material properties in the first six cases studied are shaded equally as shown in Fig. 1. As mentioned before, the felt material is assumed to be linear and isotropic.

B. Contact Condition Between a Hammer and a String

When an ideally rigid string is pushed into the top portion of a hammer, the area of contact between the string and the hammer gradually increases. The cross-sectional view of this contact is shown in Fig. 2. Originally, the string and the hammer barely touch at the origin of the coordinates. Then, the string is pushed downward by the amount d. The radius of contact, a, at x=0 is assumed to follow the formula:

$$a = (Rd)^{1/2} \tag{3}$$

where R is the radius of the string.

This formula was given by H. Hertz[4] and it is valid for a contact problem between a rigid cylinder and a semi-infinite elastic plane if d is small compared to R. Therefore, only the nodes having z-coordinate value that is smaller than the radius of contact, a, may touch the string. Also for a particular nodal point to be compressed by the string, its original y-coordinate value must be larger than the y-coordinate value of the bottom surface of the string. These values are used as concentrated loads at the nodes. The program gives the forces and displacements, stresses, and strains at each node. The total forces needed to deform the hammer by a prescribed amount is given as four times the sum of forces in the y-direction.

The above assumption of contact can be used as a rough approximation to the real string-hammer contact when studying nonlinear force-deformation relationships in a piano hammer.

III. RESULTS AND DISCUSSION

The geometries and the material properties of the first six cases studied are shown in Table I, where each area from I to V is given the same Young's modulus. Case I is considered as the standard. The geometries of A_0=0.35cm, A_1=1.75cm, B_0=0.6cm, B_1=2.0cm, and T=0.5cm were given as representative values of a bass hammer. A preliminary experiment showed that the Young's modulus of felt near the top surface is 10 times smaller than felt near the wood piece. Therefore, as the standard case of our model, E_1=1dyne/cm^2, E_2-E_4=3.16dyne/cm^2, and E_5=10.0dyne/cm^2 were used. Real values of E_1-E_5 are much larger than these values. If the real values are known to be 10^7 times larger, the force obtained from the calculation can simply be multiplied by the same ratio to estimate the force-deformation relationship of a real hammer. The radius, R=0.25cm, of the string-like piece is used for all cases. This value corresponds to an effective radius of a copper-wound steel wire used in the bass region.

The force-deformation relationship of the hammer model for the standard case is shown in Fig. 3. The calculation was performed at four different deformations in the range from d=0.0375 to 0.15cm. In Fig. 3, the circles are the calculated results and the solid line shows an approximated curve of the results using Eq. (2), with A=3.79 and B=1.67. The magnitude of B shows the order of nonlinearity of the force-deformation relationship and, in this case, it is roughly 1.67. The stiffness (the ratio of a force to a deformation) of a real hammer is practically zero for small deformations. The calculated force- deformation curve shows that the present model has this property since B is larger than 1.

It is interesting to compare the force-deformation relationship of the model with that of a real bass hammer. In our laboratory, a dynamic technique to measure the force-deformation curve was developed[2]. In this method, a hammer is accelerated by using a real piano key action to hit a rigid string-like metal piece. By measuring the acceleration of the hammer and the

force applied by the hammer to the metal piece, the force-deformation relationship is obtained. Figure 4 shows one example of the force-deformation curve of the base hammer during the compression process (that is, while the hammer is moving toward the string-like piece). The curve obtained during the relaxation process of hammer felt is usually different due to a hysteresis characteristic of felt. The circles are the measured results and the curve shows the approximation using Eq. (2) with A=1.51 and B=2.3. Unfortunately, the real hammer has a significantly higher degree of nonlinearity than the present model. Two reasons are considered for this. The first one is that the felt material has a nonlinear property which is not considered in our model. The second one is that the measurement is dynamic, whereas the present analysis is static. The effect of this difference is not known. In any case, the comparison of these results shows that the geometrial nonlinearity is only a part of the total nonlinerity of the force-deformation relationship of a real hammer. The present study is, therefore, only useful when discussing the geometrical nonlinearity.

The deformed element shapes of the hammer model for the standard case is shown in Fig. 5. Obviously, the top front elements are most severely deformed. The transition of the surface deformation from the contact to the non-contact regions between the string and the hammer is smooth. The hammer swells slightly in the thickness (z-coordinate) direction.

The following three cases show the effect of change of Young's moduli of the different material groups on the force-deformation relationship. In case II, the Young's modulus of area I is reduced to the one-half of case I. Figure 6 shows the comparison of the force-deformation curves of cases I and II. The calculated results are approximated by Eq. (2) with A=2.89 and B=1.74, indicating that case II has a larger order of nonlinearity than case I. A 50 percent decrease of Young's modulus of the outer layer causes approximately 35 to 40 percent decrease of the stiffness of the hammer. It is obvious that the hammer stiffness is signifcantly affected by the Young's modulus of the outer layer.

In case III, the Young's modulus of the elements in area II is changed to 1.78dyne/cm^2 (geometrical mean of 1.0 and 3.16), which is 56 percent of the standard case. Figure 7 shows this result. The force required to produce the same amount of deformation is approximately 80% of the force required for case I. The result of case III is approximated by A=2.88 and B=1.65 indicating the same degree of nonlinearity as case I. Figure 8 shows the result for case IV, where only the Young's modulus of group III is changed to 1.78dyne/cm^2. The effect of this change on the force-deformation curve is almost negligible as seen from the figure. It seems to be a common practice when voicing a piano to change the properties around areas II and III by adding lacquer or by releasing felt tensions with a special needle[5]. The present results show that the Young's modulus of area II is very effective in changing the stiffness of the hammer, whereas that of area III is very ineffective.

The effect that the hammer shape has on the force-deformation relationship is discussed by comparing the results of cases V and VI to those of case I. In case V, only A_1 has been changed from 1.75 (standard case) to 2.00 and, in case VI, only B_1 from 2.0 (standard case) to 1.75. The results for cases V and VI are shown in Figs. 9 and 10, respectively. When A_1 is increased, the force needed to deform the hammer by the same amount increases. The ratio of A_1 between cases I and V is approximately the same as the ratio of the forces required for the same amount of deformation. In general, it can be said that a wider hammer has a larger stiffness. When the hammer is made shorter (smaller height), the force also increases as shown by Fig. 10. In these particular cases, the ratio of B_1 between I and VI is approximately the same as the inverse of the ratio of the forces needed for the same amount of deformation. The resutls of cases V and VI are approximated by A=4.08, B=1.66, and A=4.86, B=1.70, respectively.

In all the cases discussed above, the values of B were within the range 1.65 and 1.75. This indicates that the effect of the hammer geometry and the profile of the Young's modulus on nonlinearity characteristics is not great. When we look at the results carefully, however, we notice that the degree of nonlinearity (B) is larger when the Young's modulus increases more rapidly toward the wood piece.

In order to see the effect that the increase of Young's moduli from the outer to inner layers has on nonlinear characteristics, cases VII, VIII, and IX are discussed. The Young's moduli of these cases are shown in Table II. The geometries are the same as the standard case (caseI). In cases VII and VIII, the Young's modulus gradually increases from 1.0 to 10.0 and from 1.0 to 3.16, respectively. In case IX, the Young's modulus is kept constant (=1.0) for all layers. The results of case VII has approximately the same degree of nonlinearity as case I, probably because the effective rates of increase in Young's modulus toward the wood piece are approximately the same for those two cases. The force-deformation of case VII is approximate by A=3.38 and B=1.65. When the order of the Young's modulus increase is small, the nonlinearity is also small as seen from Fig. 12. The nonlinearity index, B, of case VIII is 1.59 (with A=2.03). Another difference is that the force corrsponding to the deformation of 0.15mm is smaller than a value expected from other three forces for smaller deformations. Therefore, the approximation of the results by a curve of the form of Eq. (3) is less accurate in this case. When the Young's modulus is constant over the entire area (case IX), the nonlinearity decreases further compared to previous cases, and the constants are given as A=0.837 and B=1.43. It is clear that a larger Young's modulus increase toward the wood piece causes a larger nonlinearity. It has not been determined whether a piano hammer with a higher degree of nonlinearity is more preferable or not. At least, however, it can be said that the nonlinearity plays an important role in determining the tone of a piano. By controlling the Young's modulus profile of a hammer felt, the nonlinearity of a force- deformation relationship may also be controlled.

IV. CONCLUSIONS

The effect that the geometry and the Young's modulus profile has on the static force-deformation relationship of a piano hammer was discussed using a simplified hammer model and a finite element program. It was assumed throughout the study that the material properties of felt were istropic and linear. A hammer model with representative dimensions and the Young's modulus profile of an actual bass hammer showed a nonlinearity, B, of approximately 1.67 when the force-deformation relationship is expressed by $f = A\ d^B$. The force-deformation relationship obtained by dynamically measuring a real hammer showed a much larger nonlinearity with B=2.3 or more. The major reason for this difference seems to be the omission of the material nonlinearity. It should be mentioned, however, that even a hammer made of a material having perfectly linear properties has a great degree of geometrical nonlinearity. Due to the three-dimensional shapes of strings and hammers, the contact area between them increases at a higher rate than that of the hammer deformation.

Obviously, the Young's modulus near the top surface of the hammer is the greatest factor in determining its force-deformation relationship. The area just underneath this top surface comes next. It is interesting that the nonlinearity is also affected by changing the Young's modulus profile. It was found that a hammer with a larger Young's modulus increase toward the wood piece has a larger nonlinearity. The nonlinearities of a hammer are B=1.65 and 1.43 when a Young's modulus ratio of the innermost layer to that of the outermose layer is 10.0 (approximately linear increase) and 1.0 (uniform), respectively. A crude measurement indicated that this ratio is on the order of 10 for a real bass hammer.

The dimensional change also affects the force-deformation relationship. When the distance between the top of the wood piece and the top of the felt (B_1-B_0 in Fig. 1) is reduced, the hammer increases its nonlinearity as well as its stiffness. Also a wider hammer (a larger A_1 value in Fig. 1) has a larger stiffness. Supprisingly, however, the nonlinearity was not affected much by the change of the width.

The finite element model of a hammer used in the present study has a very simplified geometry and limited number of material properties due to the limitation of the finite element program used. However, it is hoped that a theoretical investigation of this kind, when it is combined with elegant measurement techniques, may help us to better understand the complex characteristics of a real piano hammer.

REFERENCES

1. M. Ghosh, "On the Hertzian impact of an elastic hammer on a damped pianoforte string," Phil. Mag., 7(17), 521-544 (1934).

2. H. Suzuki, "Electrical model of a hammer-string action," CBS Interim Report (April 1982, unpublished).

3. T. Yanagisawa and K. Nakamura, "Dynamic compression characteristics of piano felt," J. Acoust. Soc. Japan, 40, 725-729 (Nov. 1984).

4. H. Hertz, Hertz's Miscellaneous Papers, translated by D.E. Jones and G. A. Schott, Macmillan, New York, 146-183 (1896).

5. C. S. Robinson, "The Eclectic's Notebook, Now the Accupuncture," Piano Technicitians Jornal, 36-38 (June 1984).

CAPTIONS

Table I. Geometries and Young's moduli of a model hammer for cases I-VI.

Table II. Young's moduli of a model hammer for cases VII-IX.

Fig. 1 Finite element model of a piano hammer.

Fig. 2 Cross-sectional view of a hammer-string contact.

Fig. 3 Force-deformation relationship of the hammer model for case I.

Fig. 4 Force-deformation relationship of a real bass hammer measured by a dynamic method.

Fig. 5 Deformation of the hammer model for case I and d=0.15cm.

Fig. 6 Comparison of the force-deformation relationships between cases I and II.

Fig. 7 Comparison of the force-deformation relationships between cases I and III.

Fig. 8 Comparison of the force-deformation relationships between cases I and IV.

Fig. 9 Comparison of the force-deformation relationships between cases I and V.

Fig. 10 Comparison of the force-deformation relationships between cases I and VI.

Fig. 11 Comparison of the force-deformation relationships between cases I and VII.

Fig. 12 Comparison of the force-deformation relationships between cases I and VIII.

Fig. 13 Comparison of the force-deformation relationships between cases I and IX.

Table I. Geometries and Young's moduli of a model hammer for cases I-VI.

Case	Young's Modulus ($dyne/cm^2$)					Geometry (cm)			
	I	II	III	IV	V	A0	A1	B0	B1
I	1.0	3.16	3.16	3.16	10.0	0.35	1.75	0.6	2.00
II	~~1.0~~ 0.5	~~1.78~~ 3.16	3.16	3.16	10.0	0.35	1.75	0.6	2.00
III	1.0	~~3.16~~ 1.78	~~1.78~~ 3.16	3.16	10.0	0.35	1.75	0.6	2.00
IV	~~0.5~~ 1.0	3.16	~~3.16~~ 1.78	3.16	10.0	0.35	1.75	0.6	2.00
V	1.0	3.16	3.16	3.16	10.0	0.35	2.00	0.6	2.00
VI	1.0	3.16	3.16	3.16	10.0	0.35	1.75	0.6	1.75

Table II. Young's moduli of a model hammer for cases VII-IX.

Case	Young's Modulus (dyne/cm^2)				
	Layer 1	Layer 2	Layer 3	Layer 4	Layer 5
VII	1.0	2.0	4.0	7.0	10.0
VIII	1.0	1.41	2.0	2.65	3.16
IX	1.0	1.0	1.0	1.0	1.0

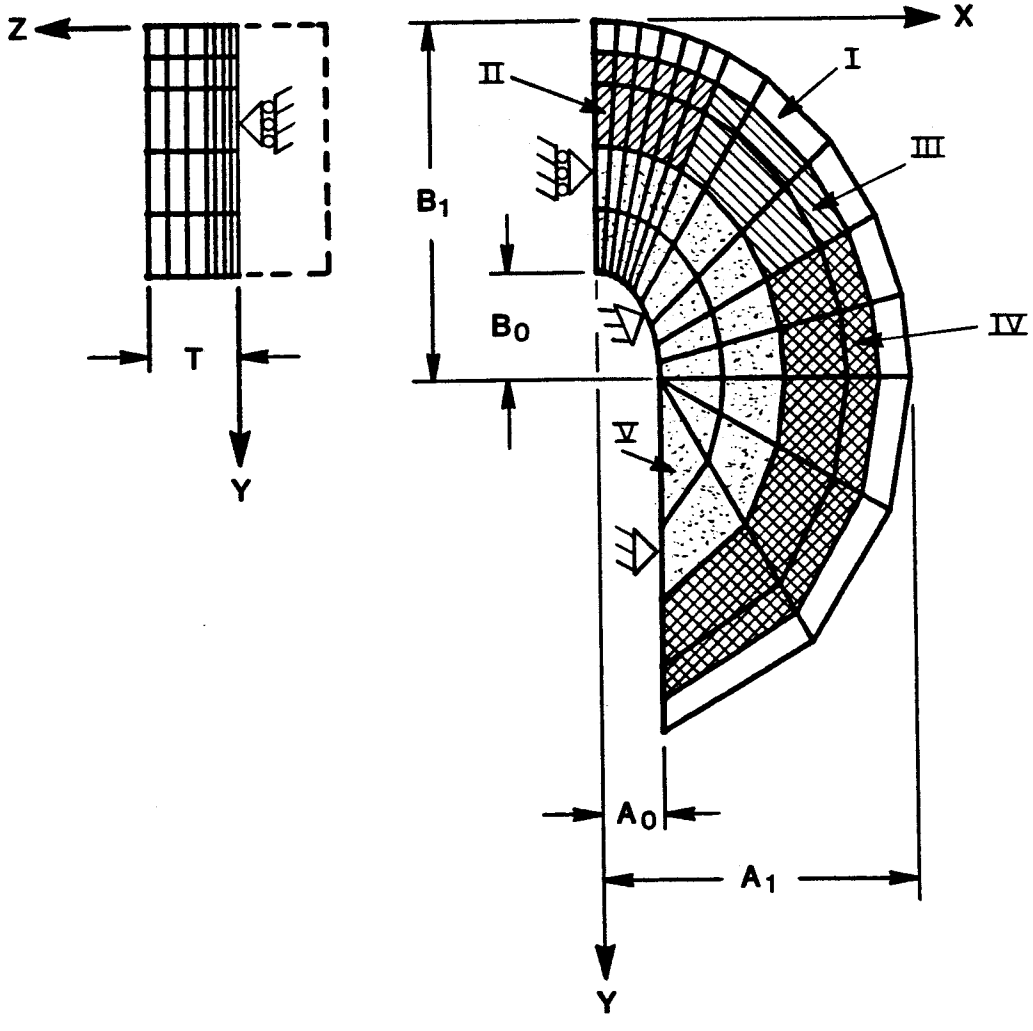

Fig. 1 Finite element model of a piano hammer.

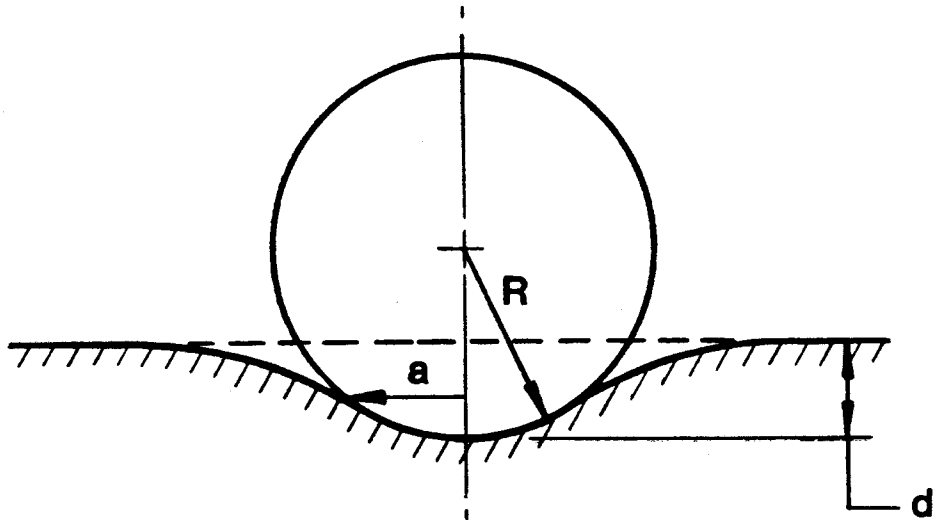

Fig. 2 Cross-sectional view of a hammer-string contact.

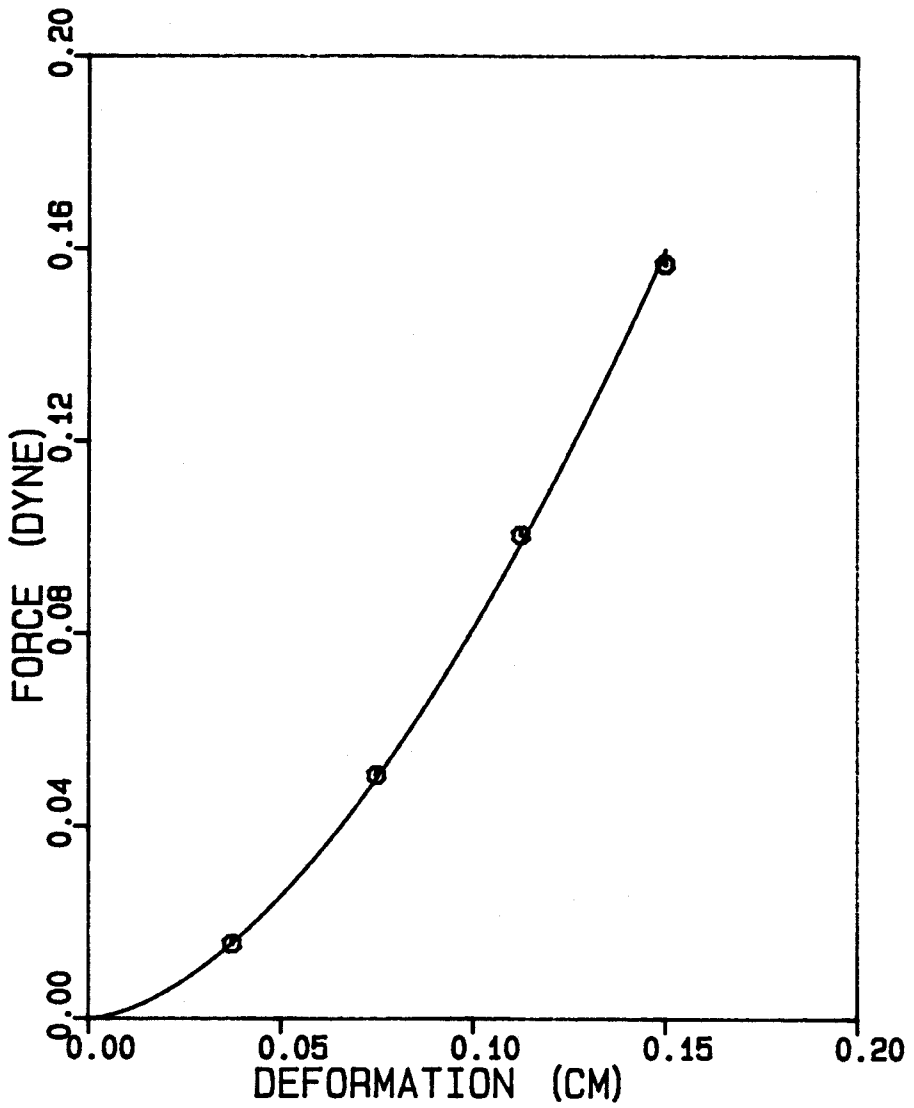

Fig. 3 Force-deformation relationship of the hammer model for case I.

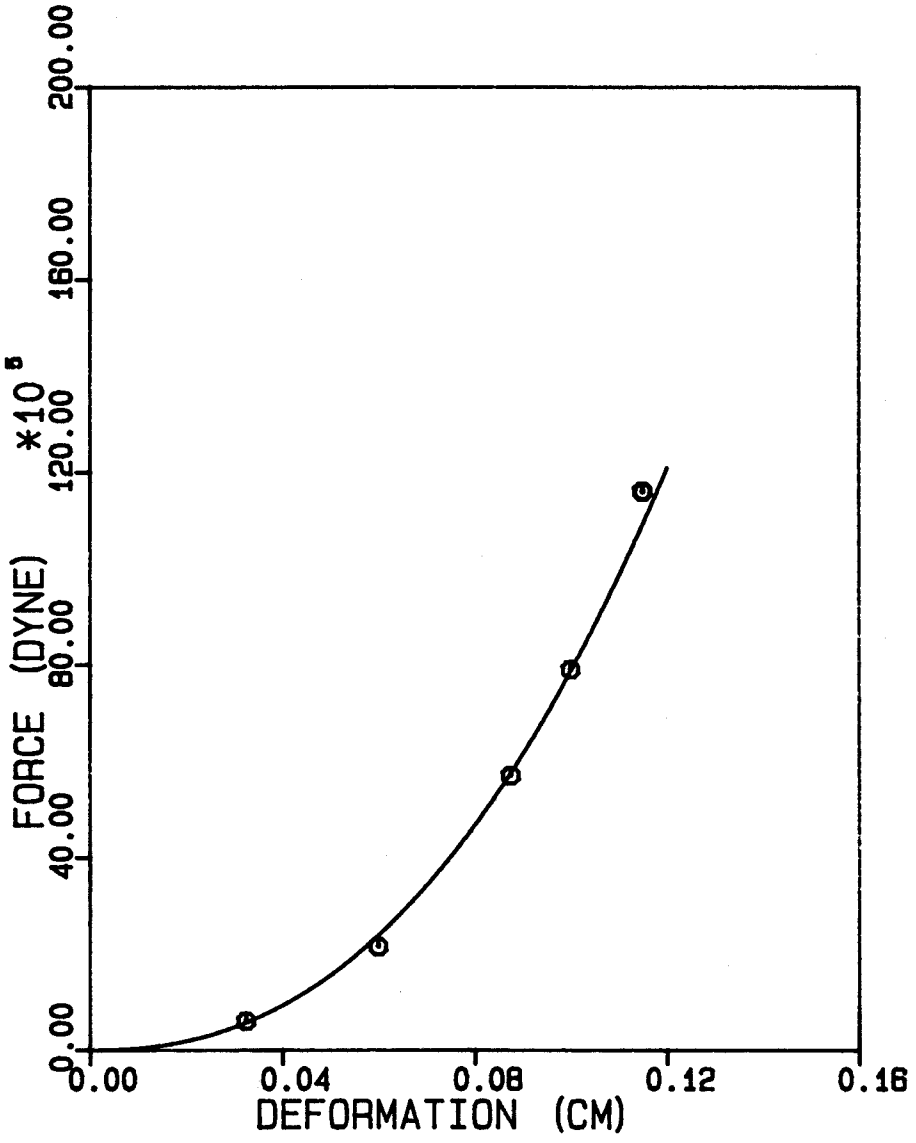

Fig. 4 Force-deformation relationship of a real bass hammer measured by a dynamic method.

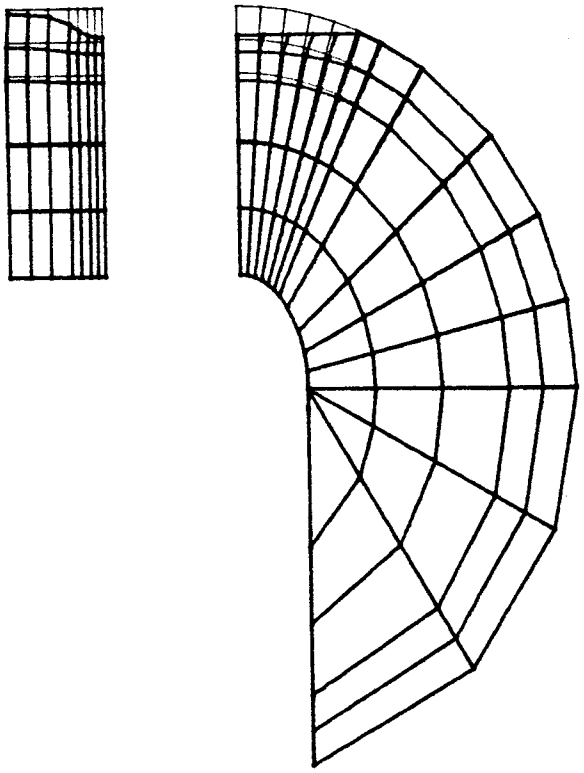

Fig. 5 Deformation of the hammer model for case I and d=0.15cm.

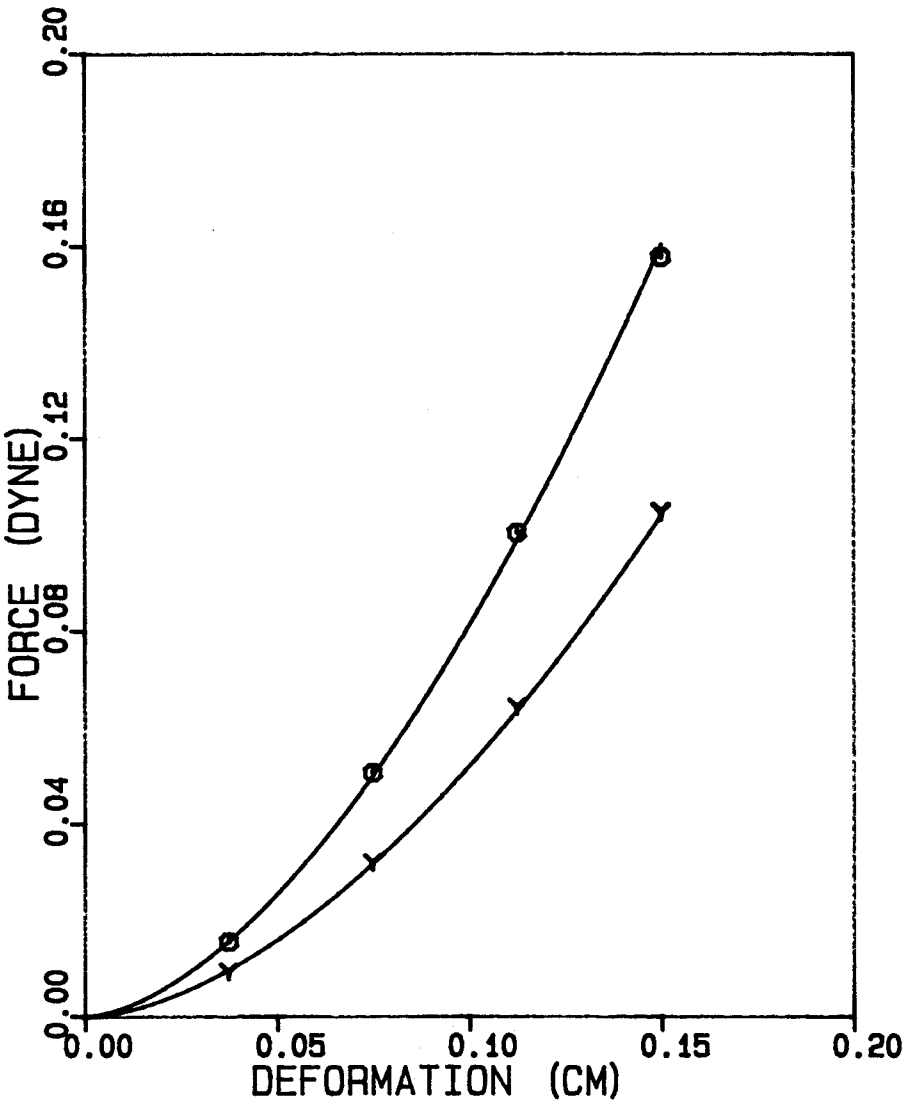

Fig. 6 Comparison of the force-deformation relationships between cases I and II.

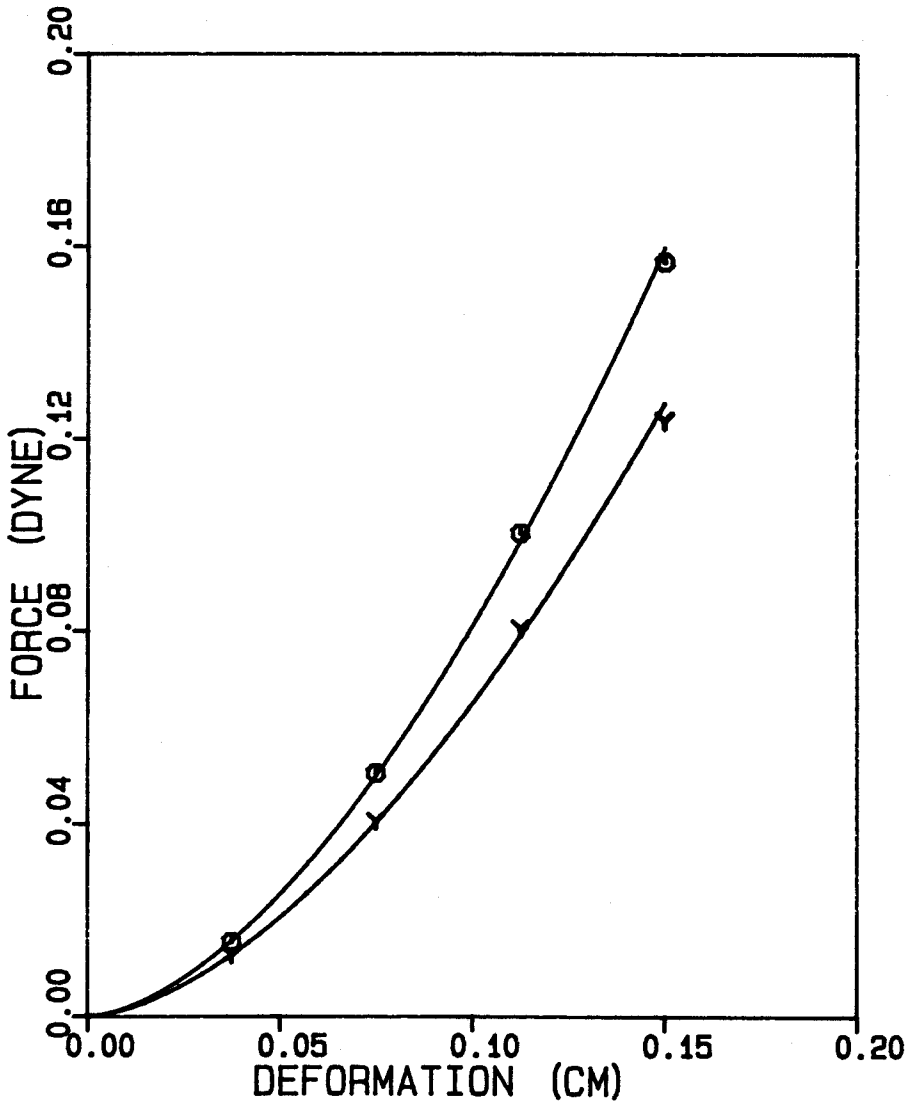

Fig. 7 Comparison of the force-deformation relationships between cases I and III.

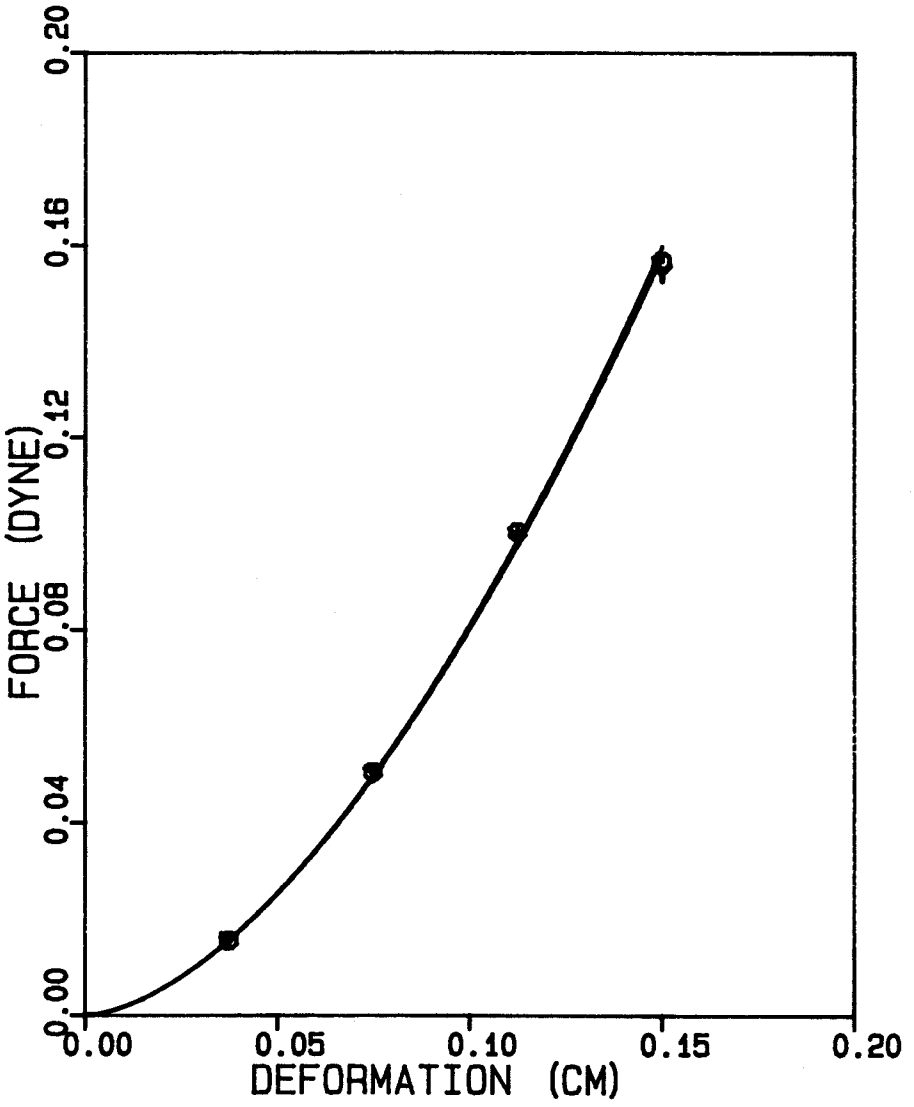

Fig. 8 Comparison of the force-deformation relationships between cases I and IV.

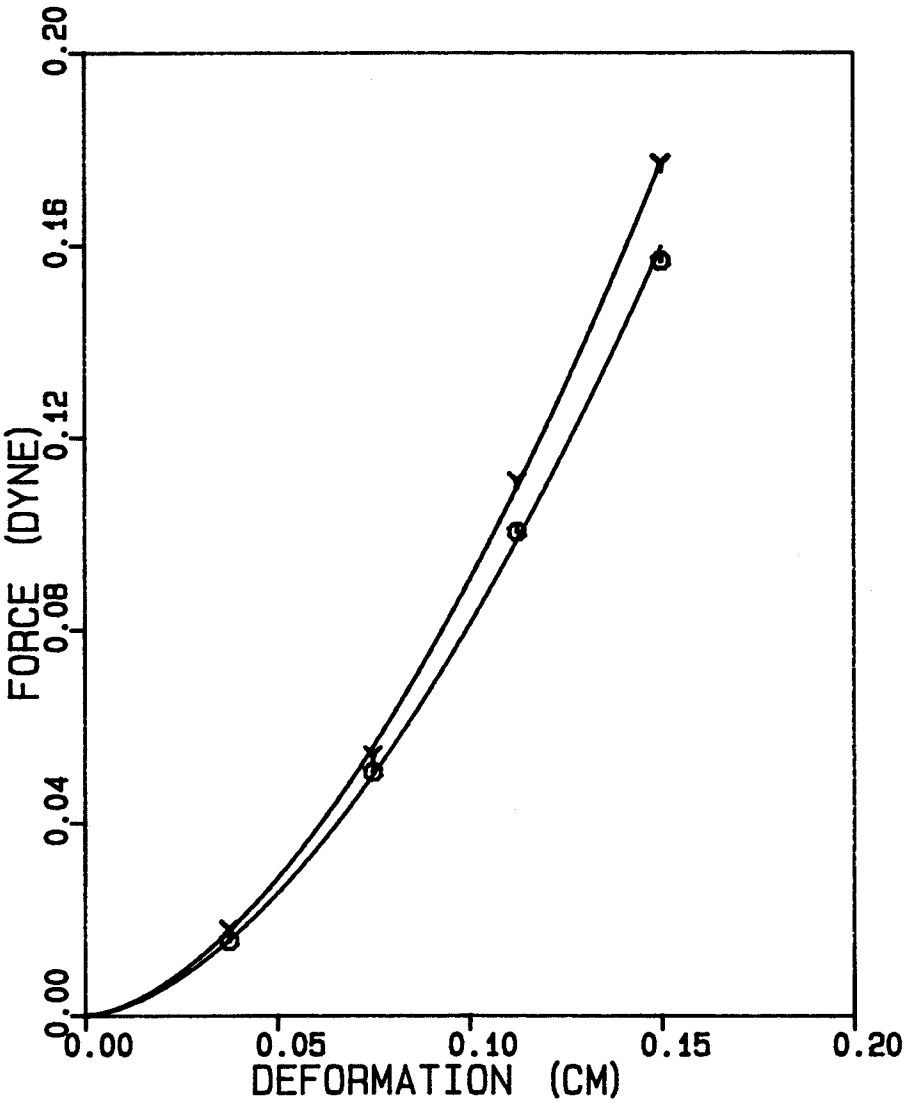

Fig. 9 Comparison of the force-deformation relationships between cases I and V.

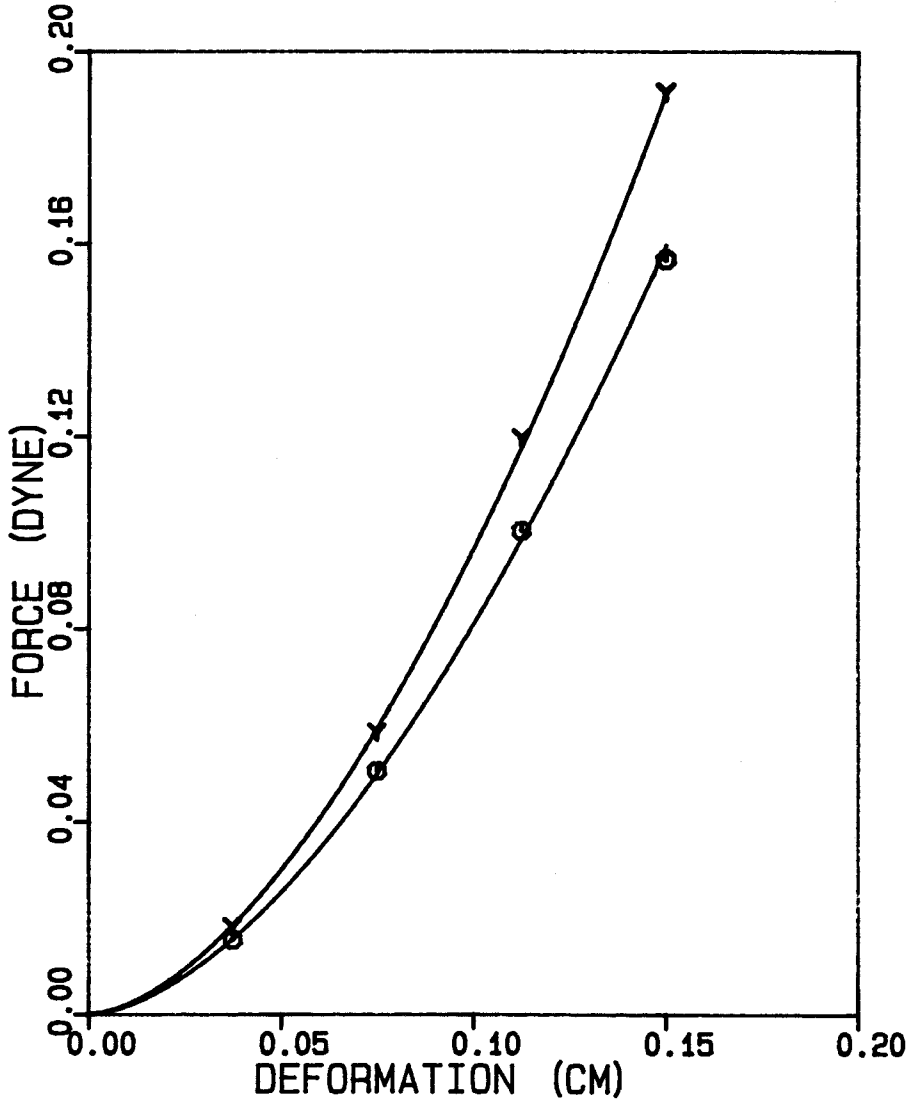

Fig. 10 Comparison of the force-deformation relationships between cases I and VI.

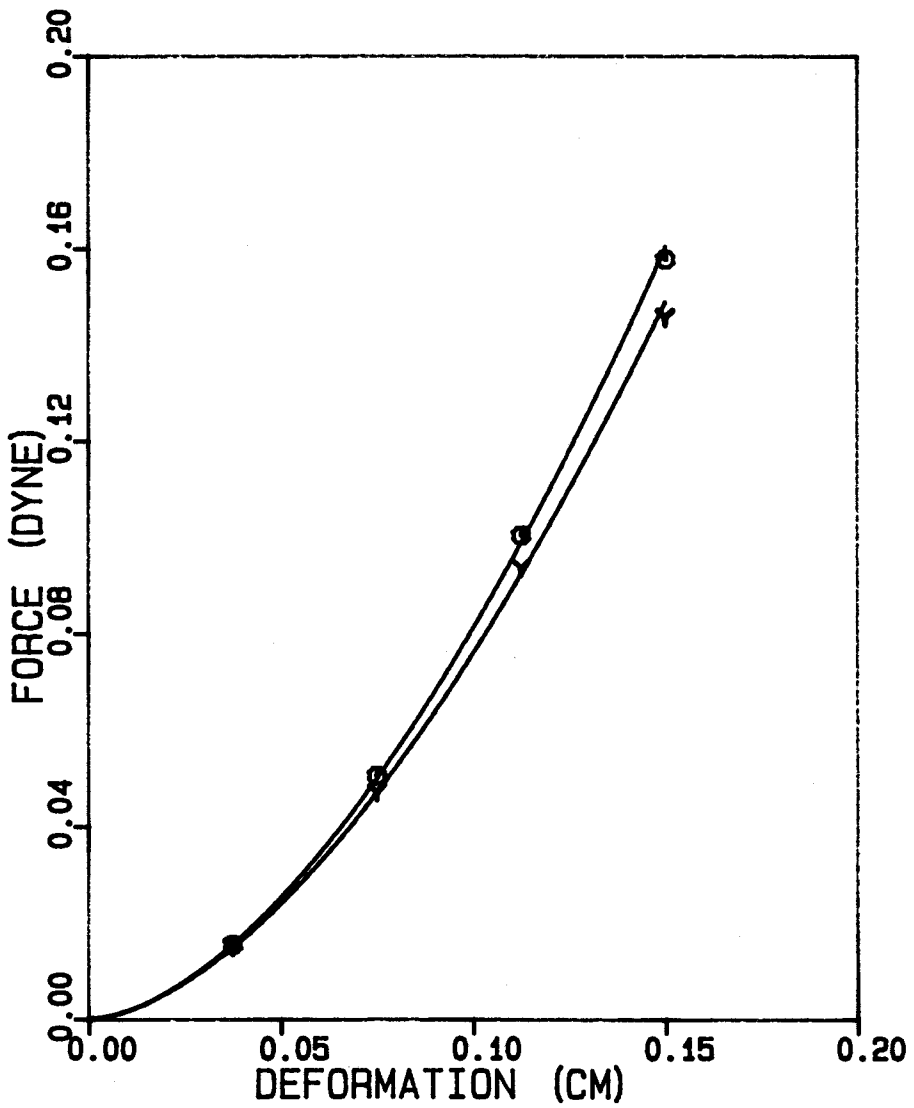

Fig. 11 Comparison of the force-deformation relationships between cases I and VII.

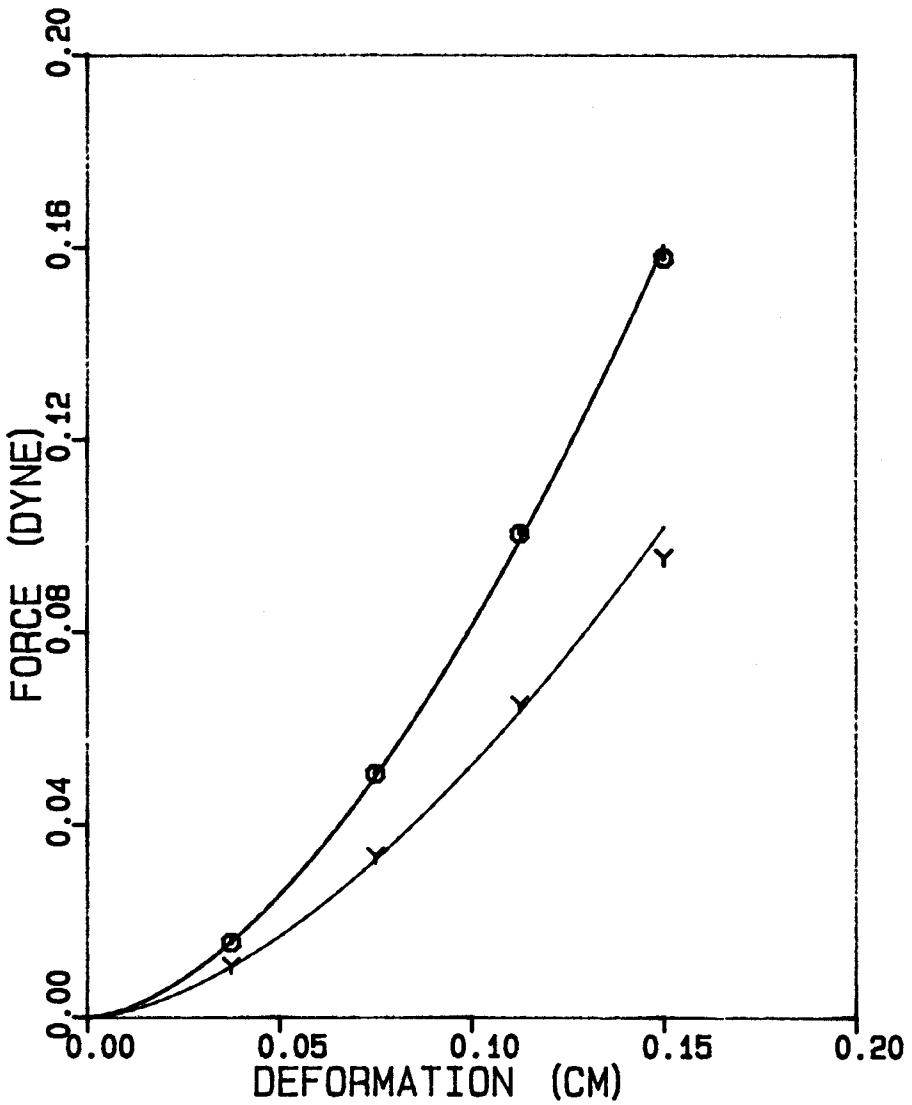

Fig. 12 Comparison of the force-deformation relationships between cases I and VIII.

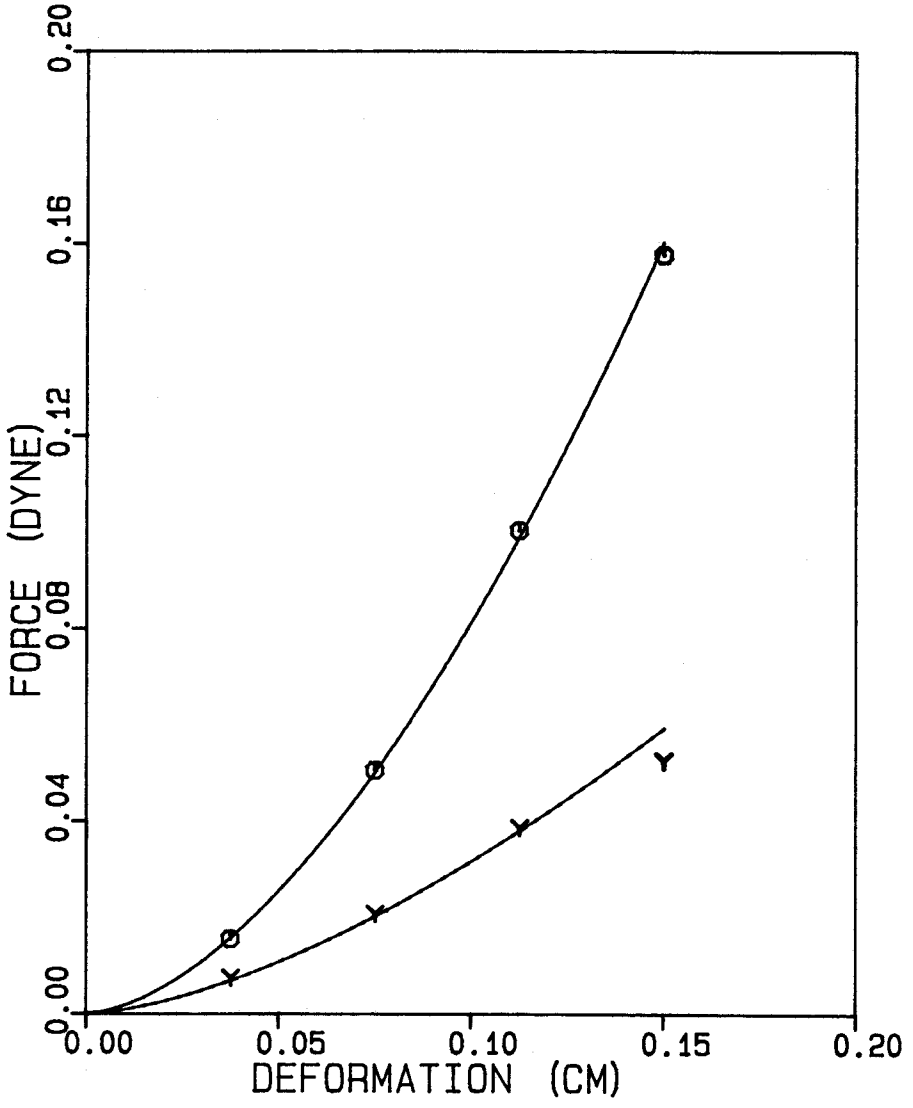

Fig. 13 Comparison of the force-deformation relationships between cases I and IX.